Assessment and Evaluation of Different Data Fusion Techniques

A. K. Helmy*, A. H. Nasr* and Gh. S. El-Taweel**
* National Authority of Remote Sensing and Space Sciences, Cairo, Egypt.
** Computer Science Dept., Faculty of Computers and Informatics, Suez Canal University, Ismailia, Egypt

Abstract- Data fusion is a formal framework for combining and utilizing data originating from different sources. It aims at obtaining information of greater quality depending upon the application. There are many data fusion techniques that can be used to produce high-resolution multispectral images from a high-resolution panchromatic (PAN) image and low-resolution multispectral (MS) images, including but not limited to, modified Intensity–hue–saturation, Brovey transform, Principal component analysis, Multiplicative transform, Wavelet resolution merge, High-pass filtering, and Ehlers fusion. One of the major problems associated with a data fusion technique is how to assess the quality of the fused (spatially enhanced) MS images. This paper represents a comprehensive analysis and evaluation of the most commonly used data fusion techniques. The performance of each data fusion method is qualitatively and quantitatively analyzed. Then, the methods are ranked according to the conclusions of the visual analysis and the results from quality budgets. An experiment based on Quickbird images shows that there is inconsistency between different performances measures used to evaluate data fusion techniques.

Keywords— Data fusion, multispectral images, quality assessment, evaluation criteria, Quick-bird images

I-INTRODUCTION

Data fusion techniques are originally devised to allow integration of different information sources, may take advantages of the complementary spatial/spectral resolution characteristics typical of remote-sensing imagery [1]. One of the major applications of remotely-sensed data obtained from earth orbiting satellites is data fusion because of repetitive coverage at short intervals from different satellites with different sensors characteristics. Data fusion is useful in such diverse applications as photo-analysis. Automated tasks, such as feature extraction and segmentation/ classification, have also been found to benefit from data fusion [2]. There is a definite need for data fusion which automatically enhances both spatial and spectral characteristics of MS and PAN images. The concept of data fusion goes back to the 1950's and 1960's, with the search for practical methods of merging images from various sensors to provide a composite image which could be used to better identify natural and manmade objects. Terms such as merging, combination, synergy, integration, and several others that express more or less the same concept have since appeared in the literature [3]. In the remote sensing community, the following definition has been adopted:

"Data fusion is a formal framework in which are expressed means and tools for the alliance of data originating from different sources. It aims at obtaining information of greater quality; the exact definition of 'greater quality' will depend upon the application" [1]. Many image fusion methods have been proposed for combining a high resolution panchromatic image (HRPI) with low resolution multispectral images (LRMIs). A detailed review on this issue was given by [4].

This paper is structured in five sections. The following section 2 explains the concept of data fusion techniques and introduces the mathematical models of several existing image fusion methods. In Section 3, the performances measures used to quantify the existing methods are analyzed. In Section 4, experiments conducted based on quick bird images are presented with their results. Finally, our conclusions are given in Section 5.

II-DATA FUSION TECHNIQUES

A variety of data fusion techniques are devoted to merge MS and PAN images which exhibit complementary characteristics of spatial and spectral resolutions [3].Such an application of data fusion is often called Pan sharpening. Several researchers have attempting to use different types of satellite images to address the data fusion problem. Several procedures of data fusion have been proposed which could aid in updating resource inventories. These methods include modified Intensity–Hue–Saturation (IHS), Brovey transform (BT), principal component analysis (PCA), Multiplicative Transform (MT), Wavelet Resolution Merge (WRM), High-Pass Filtering (HPF), and Ehlers fusion.

Data fusion approaches may be broadly characterized into several groups. Schowengerdt classified them into spectral domain techniques [5], spatial domain techniques, and scale space techniques. Ranchin and Wald classified them into three groups [6]: projection and substitution methods, relative spectral contribution methods, and those relevant to the ARSIS ' Amelioration de la Resolution Spatiale Par Injection de Structures' concept [7].

It is worth mentioning here that accurate spatial registration of the two original images is essential for most data fusion methods. This necessitates the use of geometric rectification algorithms that register the images to each other or to a standard map projection. Moreover some techniques require a radiometric balance between the two images.

1- Modified HIS

IHS can only process three bands at a time (because of using the RGB to IHS method). However, the color consistency is so good that this implementation of the approach enables images with more than three bands to be merged by running multiple passes of the algorithm and merging the resulting layers. For example, you can merge an IKONOS 4,3,2 and an IKONOS 3,2,1, and the tool automatically layer stacks 4,3,2 from the first merge with the 1 from the second to produce a merged image of all four IKONOS bands

$$\begin{bmatrix} DN_{PAN}^t \\ V1 \\ V2 \end{bmatrix} = \begin{bmatrix} \frac{1}{3} & \frac{1}{3} & \frac{1}{3} \\ \frac{-1}{\sqrt{6}} & \frac{-1}{\sqrt{6}} & \frac{2}{\sqrt{6}} \\ \frac{1}{\sqrt{6}} & \frac{-1}{\sqrt{6}} & 0 \end{bmatrix} \begin{bmatrix} DN_{MS1}^t \\ DN_{MS2}^t \\ DN_{MS3}^t \end{bmatrix} \qquad (1)$$

$$and \qquad H = \tan^{-1}[V2/V1], S = \sqrt{V1^2 + V2^2}$$

The technique works by assessing the spectral overlap between each multi-spectral band and the high resolution panchromatic band and weighting the merge based on these relative wavelengths. Therefore, it works best when merging bands where there is significant overlap of the wavelengths. As such, it may not produce good results when merging SAR imagery with optical imagery, the Modified IHS Method for Fusing Satellite Imagery was proposed by [8].

2-Brovey Transform

It is a simple method for combining data from different sensors. In this transform, three bands are used according to the following formula:

$$\begin{bmatrix} RFi_i \\ GFi_i \\ BFi_i \end{bmatrix} = \frac{PAN}{I} \times \begin{bmatrix} R_i \\ G_i \\ B_i \end{bmatrix} \qquad (2)$$

Here, R_i, G_i, and B_i are the pixel values of pixel i of each band, RF_i, GF_i, and BF_i are the pixel values of pixel i of each band that is obtained by fusion process, and $I = (R_i + G_i + B_i)/3$.
The Brovey Transform [9],[10] was developed to visually increase contrast in the low and high ends of an image's histogram (i.e., to provide contrast in shadows, water and high reflectance areas such as urban features). Consequently, the Brovey Transform should not be used if preserving the original scene radiometry is important. However, it is good for producing RGB images with a higher degree of contrast in the low and high ends of the image histogram and for producing visually appealing images. Since the Brovey Transform is intended to produce RGB images, only three bands at a time should be merged from the input multispectral scene, such as bands 3, 2, 1 from a SPOT or Landsat TM image or 4, 3, 2

from a Landsat TM image. The resulting merged image should then be displayed with bands 1, 2, 3 to RGB.

3-Principal Component Analysis

The major goal of this method is to retain the spectral information of the multispectral images. This algorithm is mathematically rigorous [11]. It is assumed that:

- PC-1 contains only overall scene luminance; all inter-band variation is contained in the other PCs, and
- Scene luminance in the Short Wave Infra Red (SWIR) bands is identical to visible scene luminance.

With the above assumptions, the forward transform into PCs is made. PC-1 is removed and its numerical range (min to max) is determined. The high spatial resolution image is then remapped so that its histogram shape is kept constant, but it is in the same numerical range as PC-1. It is then substituted for PC-1 and the reverse transform is applied. This remapping is done so that the mathematics of the reverse transform do not distort the thematic information

$$\begin{bmatrix} Pc1 \\ pc2 \\ ... \\ pc_n \end{bmatrix} = \begin{bmatrix} v11 & v21 & ... & vn1 \\ v12 & v22 & ... & vn2 \\ ... & ... & ... & ... \\ v1n & v2n & ... & vnn \end{bmatrix} = \begin{bmatrix} DN_{MS1}^l \\ DN_{MS2}^l \\ ... \\ DN_{MSn}^l \end{bmatrix} \qquad (3)$$

The (PCA) method is best used in applications that require the original scene radiometry (color balance) of the input multispectral image to be maintained as closely as possible in the output file. As this method scales the high resolution data set to the same data range as PC-1, before the Inverse Principal Component calculation is applied, the band histograms of the output file closely resemble those of the input multispectral image. Unfortunately, this radiometric accuracy comes at the price of a large computational overhead. The (PCA) method is slow and requires the most system resources. Its output file tends to have the same data range as the input multispectral file.

4-Multiplicative Transform

This method uses a simple multiplicative algorithm:
$$(DN_{low-resolution})(DN_{high-resolution}) = DN_{fused-image} \qquad (4)$$

The algorithm is derived from the four component technique of [12]. It is argued that of the four possible arithmetic methods to incorporate an intensity image into a chromatic image (addition, subtraction, division, and multiplication), only multiplication is unlikely to distort the color. First the intensity component is removed via band ratios, spectral indices, or PC transform. The result is an increased presence of the intensity component. For many applications, this is desirable. People involved in urban or suburban studies, city

planning, and utilities routing often want roads and cultural features (which tend toward high reflection) to be pronounced in the image.

This method is computationally simple; it is generally the fastest method and requires the least system resources. However, the resulting merged image does not retain the radiometry of the input multispectral image. Instead, the intensity component is increased, making this technique good for highlighting urban features (which tend to be higher reflecting components in an image).

5-Wavelet Resolution Merge

The basic theory of Wavelet Resolution Merge (WRM) is that an image can be separated into various high- and low-frequency components using various high- and low-pass filters. The wavelet family can be thought of as a high-pass filter. Thus wavelet-based high- and low-frequency images can be created from any input image. By definition, the low-frequency image is of lower resolution and the high-frequency image contains the detail of the image.

This process can be repeated recursively. The created low-frequency image could be again processed with the kernels to create new images with even lower resolution. Thus, starting with a 5-meter image, a 10-meter low-pass image and the corresponding high-pass image could be created. A second iteration would create a 20-meter low- and, corresponding, high-pass images. A third recursion would create a 40-meter low- and, corresponding, high-pass images, etc.

Using wavelets, one can decompose the 5-meter image through several iterations until a 40-meter low-pass image is generated plus all the corresponding high-pass images derived during the recursive decomposition. This 40-meter low-pass image, derived from the original 5-meter pan image, can be replaced with the 40-meter multispectral image and the whole wavelet decomposition process reversed, using the high-pass images derived during the decomposition, to reconstruct a 5-meter resolution multispectral image. The approximation component of the high spectral resolution image and the horizontal, vertical, and diagonal components of the high spatial resolution image are fused into a new output image. If all of the above calculations are done in a mathematically rigorous way, one can derive a multispectral image that has the high-pass (high-frequency) details from the 5-meter image [13]-[15] In this scenario, it should be noted that the high-resolution image (panchromatic) is a single band and so the substitution image, from the multispectral image, must also be a single band. There are tools available to compress the multispectral image into a single band for substitution using the IHS transform or PCA transform. Alternately, single bands can be processed sequentially.

Multisensor image fusion is a tradeoff between the spectral information from LRMI sensor and the spatial information from an HRPI sensor. With the wavelet transform fusion method, it is easy to control this tradeoff [16].

6 High-Pass Filtering

Improving wavelet-based Resolution Merge functionality led to advancement of the High Pass Filtering (HPF) add-back method to the level at which it yields results comparable to redundant wavelets but with much smaller computation time and data space requirements.

The general algorithm [17], [18] is;

a) The ratio between multispectral cell size to high-resolution cell size is calculated for quick bird imagery, R=4

b) Then HPF of high spatial resolution image is derived. This operation produces the HPF image. A high pass convolution filter kernel (HPK) is created and used to filter the high-resolution input data. The size of the HPK is a function of the relative input pixel sizes, R. All values of the kernel are set to –1 except the center value. There are three possible values for the kernel center value. The lowest of the three values for each kernel size is the default.

c) Resample the multi-spectral image to the pixel size of the high-pass image. The low spatial resolution image is resampled to the pixel size of the high resolution image using a bilinear algorithm (4 nearest neighbors). The resulting image will, therefore, have the same pixel size as the high resolution image.

d) Add the HPF image to each multi-spectral band. The value of the weight W applied to the HPF image, prior to addition to the multi-spectral image, depends on both R and the standard deviations (SD) of both the HPF image and multi-spectral band. In addition, the weight is allowed to vary so you can adjust the crispness of the result. The calculation for each band of the input image will then be:

Pixel (out) = [Pixel (in)] + [HPF x W]

e) Stretch the new multi-spectral image to match the mean and standard deviation of the original (input) multi-spectral image.

7-Ehlers Fusion

The first step is to transform the low resolution multispectral image into an Intensity-Hue-Saturation (IHS) image working with three selected bands (RGB). Next, the panchromatic image P and the intensity component I are transformed into the spectral domain using a two-dimensional Fast Fourier Transform (FFT). The power spectrum of both images is used to design the appropriate low pass filter (LP) for the intensity component and high pass filter (HP) for the high resolution panchromatic image. Based on the ratio of pixel sizes between the high and low resolution images, cut-off frequencies for these filters can be established [19]. Filtering will be directly performed in the frequency domain as it involves only multiplications. An inverse FFT transforms both components back into the spatial domain. The low pass filtered intensity (I^{LP}) and the high pass filtered panchromatic band (P^{HP}) are added and matched to the original intensity histogram. At the end, an inverse IHS transform converts the fused image back into the RGB domain

III- EVALUATION CRITERIA FOR DATA FUSION TECHNIQUES

In the preceding section, the mathematical models of the seven methods were expressed. The performances of each method will be assessed by comparison to a reference. Then, the methods will be ranked according to the conclusions of the visual analysis and the results from quality budgets. We will use the consistency property recommend by [20] which states that any synthetic image, once degraded to its original resolution, should be as close as possible to the original image. In other words, spatial degradation of the fused image should lead to the original image or close. Consistency, however, is a necessary condition, and its fulfillment does not imply a correct fusion. Many of the methods tested during this contest use multi-scale approaches in order to inject high spatial frequency components while preserving low spatial frequency components. Fusion methods adopting such approaches usually check this property [7]. When reference MS images are available for comparisons with fusion results, assessment of fidelity to the reference usually requires computation of a number of different indices as indicated below.

1- Average Correlation Coefficients (CC)

The correlation between each band of the fused image and reference MS images is calculated. Lower value of correlation indicates higher spectral distortion and vice versa.

2- Bias in the Mean and standard deviation

The bias between fused and MS image indicate the amount of deviation of the fused image.

3- Root Mean Square Error (RMSE)

The comparison is also made on the basis of the mean squared error (MSE) between the true MS images and the fused images.

$$RMSE = \sqrt{\frac{\sum (f_i - f_i')^2}{mn}} \qquad (5)$$

Where n and m are number of pixels, f_i represents the true MS image intensity value at the ith pixel and f_i is the corresponding fused MS image intensity.

4- Average angle error

Given two spectral vectors v and v_f, both having L components, in which $v = \{v_1, v_2, . . . , v_L\}$ is the original spectral pixel vector, while $v_f = \{v1, v2, . . . , v_L\}$ is the distorted vector obtained by applying fusion to the coarser resolution MS data, the Spectral Angle Mapper (SAM) denotes the absolute value of the spectral angle between the two vectors.

$$SAM (v, \hat{v}) = \arccos(\frac{(v, \hat{v})}{\|v\| \|\hat{v}\|}) \qquad (6)$$

A value of SAM (1) equal to zero denotes absence of spectral distortion, but radiometric distortion is possible (the two pixel vectors are parallel but have different lengths). SAM is measured in either degrees or radians and is usually averaged over the whole image to yield a global measurement of spectral distortion.

5- Relative dimensionless global error in synthesis (ERGAS)

Error index offers a global picture of the quality of the fused product. This is given by:

$$ERGAS = 100 \frac{d_h}{d_l} \sqrt{\frac{1}{L} \sum_{l=1}^{L} \left(\frac{rmse(l)}{\mu(l)} \right)^2} \qquad (7)$$

d_h/d_l is the ratio between the pixel sizes of Pan and MS, e.g., 1/4 for Ikonos and QuickBird data.
$\mu(l)$ is the mean (average) of the lth band,
L is the number of bands.
The ideal value of ERGAS is zero.

6- Quality index Q4

$Q4$ [21], [22] is obtained through the use of correlation coefficient CC between hyper-complex numbers, quaternion, representing spectral pixel vectors. $Q4$ is made of three different factors: The first is the modulus of the hyper-

complex CC between the two spectral pixel vectors and is sensitive to both the loss of correlation and to spectral distortion between the two MS data sets. The second and third terms, respectively, measure contrast changes and mean bias on all bands simultaneously.

The modulus of the hyper-complex CC measures the alignment of the spectral vectors. Therefore, its low value may be detected when radiometric distortion is accompanied by spectral distortion. Thus, both radiometric and spectral distortions may be encapsulated in a unique parameter.

All statistics are calculated as averages on $N \times N$ blocks, either $N = 16$ or $N = 32$. Eventually, $Q4$ is averaged over the whole image to yield the global score index. The highest value of $Q4$, attained if and only if the test MS image is equal to the reference, is one; the lowest value is zero.

IV- EXPERIMENTAL RESULTS AND EVALUATIONS

In order to validate the theoretical analysis, the performance of the representative methods discussed above was further evaluated by experimentation. A quick-bird panchromatic image HRPI (455–900 nm) of 0.7-m resolution and the red (631.9–697.7 nm), green (520–600 nm), blue (450–520 nm) and NIR (760–890 nm) bands of the 2.8-m resolution LRMIs were used in this experiment. The images cover the area of the pyramid, Cairo, Egypt acquired on 2000. The pair of images was geometrically registered to each other after being resampled to 0.7 m resolution using cubic convolution technique. Quick-bird data was collected at 11 bits per pixel (2048 gray tones). This means that there is more definition in the gray scale values and the viewer can see more detail in the image. In order to benefit from this additional information, the processing and evaluation were entirely based on the original 11-bit data and the data was converted to eight-bit for display purposes only. Fig. 1 shows the HRPI. and the natural color image of the original LRMIs (red–green–blue combination) is shown in Fig. 2. The NIR band is not shown but was processed and numerically evaluated as well. The study area is composed of various features such as cars, buildings, trees, lawn, etc., ranging in size from less than 1 m up to 100 m. It is obvious that the HRPI has better spatial resolution than the LRMIs and more detail can be seen from the HRPI. Table-3 gives the correlation coefficients (CCs) between the HRPI (down-sampled to 2.8-m pixel size) and the original LRMIs, which show that the CC of the NIR band is comparable with the CCs of other bands, indicating that the Quick-bird NIR band is very important to the Quick-bird PAN band as the other bands.

Table 3. Correlation Coefficients for the Quick-Bird HRPI (Resampled at 4-m Pixel Size) and the Original LRMIS

red	green	blue	NIR
0.906	0.934	0.935	0.919

The modified IHS and Brovey Transform methods can only handle three bands. In order to evaluate the NIR band as well, we selected the red–green–blue combination for true natural color and the NIR–red–green combination for false color. The resolution ratio between the Quick-bird HRPI and the LRMIs is 1: 4. Therefore, in the HPF resolution merge a 5 X 5 boxcar filter was used.

The fused results of the PCA, Multiplicative, Brovey, Modified HIS, HPF, WRM, and Ehlers methods are displayed in Figs. 3–9, respectively. Since the results are too large to be assessed together, for better evaluation, Fig. 10 shows sub-scenes from the original natural color composite and the corresponding results together. The performance of each fusion method should be evaluated in terms of the quality of the degraded fused image compared with the original LRMIs. It should be as identical as possible.

Fig. 1. Original HRPI (panchromatic band).

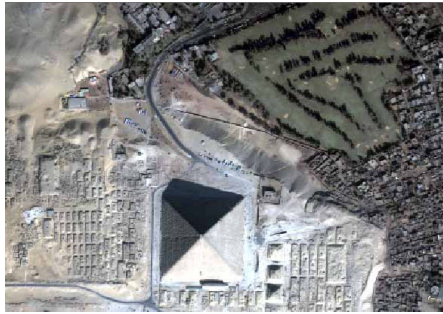Fig. 2. Original LRMIs (RGB)
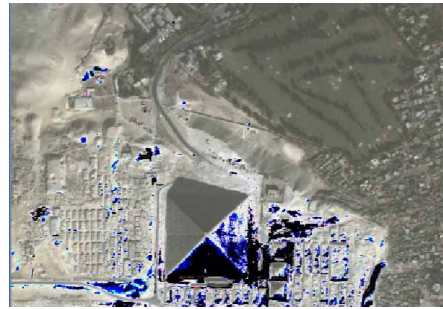
Fig. 3. Result of the PCA Method.

Fig. 4. Result of the Multiplicative Method

Fig. 5. Result of the Brovey Method

Fig. 6. Result of the modified IHS

Fig. 7. Result of the HPF Method

Fig. 8 Result of WRM Method

Fig. 9. Result of Ehlers Method.

Fig. 10. Subscenes of the original LRMIs, HRPI and the fused resulting HRMIs by different methods (double zoom). (Left to right sequence, row by row). Original LRMIs, Original HRPI, PCA, Multiplicative, Brovey, HIS, HPF, WRM, and Ehlers.

Visual inspection provides an overall impression of the detailed information and the similarity of the original and resultant images. Comparing the spatial quality of all the resultant images (Figs. 3–9) with that of the original images (Figs. 1-2) visually, it is obvious that the spatial resolutions of the resultant images are higher than that of the original images. Some small features such as building edges, which were not interpretable in the original image, can be identified individually in each of the resultant images. Trees and buildings are much sharper in the resultant images than in the original images. It is easy to see this effect in Fig. 10. This means that all of the used methods can improve spatial quality via the fusion process. In figures

4 and 6 multiplicative and HIS methods produce a significant color distortion with respect to the original LRMSI. In Fig. 3 the PCA methods produce noticeable color distortion with respect to the original image, however it looks better. In Figs. 7 and 8, the HPF and WRM methods produce color distortion in instances such as water bodies and vegetated areas. In Fig. 7, the HPF method also exhibits slight color distortion, as in the bright built up area, for instance, but better than WRM methods (see also Fig. 10). This may be due to the large ripple outside its band-pass in the frequency response of its low-pass filter.

Nevertheless the Ehlers method looks better than all of the other methods in terms of the quality of spectral information.

The HPF and WRM methods look sharper than the others. However, this is probably due to over-enhancement along the edge area because these additive methods have not considered the differences in high-frequency information between the panchromatic band and the multispectral bands, so this should not be considered as a merit of the HPF and WRM methods. The quality of spectral information is the principal criterion. In Fig. 10, it can be seen that the Ehlers method also gives better spatial quality than the HPF method. Overall, it is obvious by visual inspection that the Ehlers method gives the synthesized result closest to what the corresponding multi sensors would observe at the high-resolution level.

In addition to the visual analysis, the performance of each method was further quantitatively analyzed by checking the (next or following) seven properties. The correlation coefficient (CC), bias in mean, bias in standard deviation, Root mean squared error (RMSE) between the original MS images and the fused images, SAM, ERGAS, and Q4.

ERGAS and Q4 indicate the evidence of quality in terms of spatial details, while the RMSE, SAM, bias in mean, bias in standard deviation and correlation values reflect the fidelity

of spectral information. For example, the RMSE, bias in mean, SAM, and ERGAS should be as low as possible. On the contrary, the higher the correlation coefficient and Q4 are, the better the fusion is. The obtained results are summarized in Table 4.

Table 4. Quantitative Assessment of the Fusion Results Provided By the Considered Techniques Applied To the Quick Bird Data Set: (A) Band 2, (B) Band 3, (C) Band 4 (The IHS and BT Techniques Have Been Applied To Bands 2, 3, and 4 False-Color Compositions)

	CC	Mean bias	standard deviation (bias)	RMSE	SAM	ERGAS	Q4
PCA	0.9	24.9	34.9	5.92	**2.4**	3.5	0.9
Multiplic	0.43	62.05	44.6	13.8	6.1	7.3	0.4
B. T.	0.87	75.19	53.3	9.13	4.1	3.8	0.84
HIS	0.89	44.9	35.7	7.03	3.7	4.9	**0.96**
HPF	0.89	**20.09**	15.7	3.2	4.7	2.65	0.92
WRM	0.92	72.32	**9.28**	**2.1**	3.8	2.72	0.9
Ehlers	**0.93**	56.7	68.3	5.42	2.65	**1.354**	0.91

As can be observed from the table, the measures used to evaluate data fusion techniques can be divided into two groups, group indicate the spectral characteristics of fused image including CC, bias in mean, bias in standard deviation, RMSE, and SAM. The other one measure the spatial characteristics including ERGAS and Q4.

Firstly regardless of spectral evaluation, as correlation coefficients between original LRMIs and fused images go high, it is an indication that the fused image exhibits same spectral characteristics as original image. It is clear that Ehlers followed by WRM have the highest correlation values. On the other hand HPF shows smallest shift, bias in mean, between original and fused images distribution followed by PCA. While Wavelet Resolution Merge introduces the best curve fitting, standard deviation bias, between the two distributions of original and fused images, also it provides the best value of RMSE. SAM which indicate the absence of spectral distortion, PCA comes with the best value followed by HIS As can be seen from the results of spectral evaluation using the previous measures, there is a conflict between the measures, this is due to the following:

Bias in mean and stander deviation give an over all imagery of the distribution between original and fused images, distortion of fused image is not noticeable due to engage in recreation of these measures.

CC is insensitive to a constant gain and bias between two images and does not allow subtle discrimination of possible fusion artifacts.

SAM with value of zero, denotes absence of spectral distortion, but radiometric distortion is possible (the two pixel vectors are parallel but have different lengths).

Secondly regardless of spatial evaluation, ERGAS measure shows that Ehlers is the best followed by HPF and WRM while Q4 introduce HIS as the best one followed by HPF. Again there is a conflict between which technique is the best. The reason of this conflict due to:

ERGAS offers a global picture of the quality of the fused product. It depends upon mean and RMSE of each band which introduce vagueness indications.

Although Q4 measures the alignment of the spectral vectors (its good when radiometric distortion is accompanied by spectral distortion). All statistics are calculated as averages on $N \times N$ blocks. Eventually, $Q4$ is averaged over the whole image to yield the global score index. This average process may introduce uncertainty results.

CONCLUSION

The performance of many existing image fusion techniques including, modified Intensity–Hue–Saturation (IHS), Brovey Transform (BT), Principal Component Analysis (PCA), Multiplicative Transform (MT), Wavelet Resolution Merge (WRM), High-Pass Filtering (HPF), and Ehlers fusion, are assessed and evaluated. Visual and objective performance evaluations of the used techniques have been conducted using Quickbird data. Both spectral and spatial qualities of the fused products were assessed. It can be concluded that; From experimental results, by combination of the visual inspection results and the quantitative results, it is possible to see that there is inconsistency between the different used measures. The visual analysis has been confirmed by the quantitative evaluation.

REFERENCES

[1] Wald, L. Some terms of reference in data fusion, IEEE Trans. Geosci. Remote Sens., vol. 37, no. 3, pp. 1190–1193.,1999.

[2] Bruzzone, L., L. Carlin, L. Alparone, S. Baronti, A. Garzelli, and F. Nencini, Can multiresolution fusion techniques improve classification accuracy, Proc. SPIE, vol. 6365, ID no. 636509., 2006.

[3] Wang, Z., D. Ziou, and C. Armenakis, A comparative analysis of image fusion methods, IEEE Trans. Geosci. Remote Sens., vol. 43, no. 6, pp. 1391–1402, 2005.

[4] Pole, C. and J. L. Van Genderen, Multi-sensor image fusion in remote sensing: Concepts, methods, and applications, Int. J. Remote Sen., Vol. 19, No. 4, pp. 743-757, 1998.

[5] Schowengerdt, R. A., *Remote Sensing: Models and Methods for Image Processing*, 2nd ed. Orlando, FL: Academic, 1997.

[6] Ranchin, T. and Wald L., Fusion of high spatial and spectral resolution images: the ARSIS concept and its implementation. Photogrammetric Engineering and Remote Sensing, vol. 66, no.1, pp. 49-61, 2000.

[7] Ranchin, T., Aiazzi B., Alparone L., Baronti S., Wald L., Image fusion. The ARSIS concept and some successful implementation schemes. ISPRS Journal of Photogrammetry & Remote Sensing, vol. 58, pp. 4-18, 2003.

[8] Siddiqui Y., The Modified IHS Method for Fusing Satellite Imagery, In ASPRS Annual Conference Proceedings, 2003.

[9] Liu, J. G., Smoothing filter-based intensity modulation: A spectral preserve image fusion technique for improving spatial details, *Int. J. Remote Sens.*, vol. 21, no. 18, pp. 3461–3472,2000

[10] Gillespie, A. R., A. B. Kahle, and R. E. Walker, Color enhancement of highly correlated images—II. Channel ratio and 'chromaticity' transformation techniques, *Remote Sens. Environ.*, vol. 22, pp. 343–365, 2003.

[11] Béthune, S., F. Muller, and J. P. Donnay, Fusion of multi-spectral and panchromatic images by local mean and variance matching filtering techniques, *Fusion of Earth Data*, 1998.

[12] Crippen, R.E., A Simple Spatial Filtering Routine for the Cosmetic Removal of Scan-Line Noise from Landsat TM P-Tape Imagery. Photogrammetric Engineering & Remote Sensing vol. 55, no. 3, pp. 327-331, 1989.

[13] King, Roger and Wang, Jianwen, A Wavelet Based Algorithm for Pan Sharpening Landsat 7 Imagery, 2001

[14] Lemeshewsky, G. P, Multispectral multisensor image fusion using wavelet transforms, in Visual Image Processing VIII, S. K. Park and R. Juday, Ed., Proc SPIE 3716, pp. 214-222, 1999

[15] Lemeshewsky, G. P, personal communication, Lemeshewsky, G.P., "Multispectral Image sharpening Using a Shift-Invariant Wavelet Transform and Adaptive Processing of Multiresolution Edges" in Visual Information Processing XI, Z. Rahman and R.A. Schowengerdt, Eds., Proc SPIE, vol. 4736, 2002

[16] Zhou, J., D. L. Civco, and J. A. Silander, A wavelet transform method to merge Landsat TM and SPOT panchromatic data, Int. J. Remote Sen., vol. 19, no. 5, pp. 823-854, 1998

[17] Schowengerdt, R. A., Reconstruction of multi-spatial, multi-spectral image data using spatial frequency content, Photogramm. Eng. Remote Sens., vol. 46, no. 10, pp. 1325–1334, 1980.

[18] Aiazzi, B., L. Alparone, S. Baronti, and A. Garzelli, Context-driven fusion of high spatial and spectral resolution images based on oversampled multi-resolution analysis, *IEEE Trans. Geosci. Remote Sens.*, vol. 40, no. 10, pp. 2300–2312, 2002.

[19] Ehlers, M., Multisensor image fusion techniques in remote sensing, *ISPRS J. Photogramm. Remote Sens.*, vol. 46, no. 1, pp. 19–30,1991.

[20] Thomas, C. and L. Wald, Comparing distances for quality assessment of fused products, in Proc. 26th EARSeL Annu. Symp. New Develop. Challenges Remote Sens., Warsaw, Poland. Z. Bochenek, Ed., Rotterdam, The Netherlands: Balkema, pp. 101–111, 2007.

[21] Alparone, L., S. Baronti, A. Garzelli, and F. Nencini, A global quality measurement of Pan-sharpened multispectral imagery, IEEE Geosci. Remote Sens. Lett., vol. 1, no. 4, pp. 313–317, 2004.

[22] Thomas, C. and L. Wald, An MTF-based distance for the assessment of the geometrical quality of fused products, in *Proc. 9th Int. Conf. Inf. Fusion*, Florence, Italy, pp. 1–7, 2006.